Antibacterial activity and mechanism of sanguinarine against *Providencia rettgeri in vitro* (#45027)

First submission

Guidance from your Editor

Please submit by **24 Feb 2020** for the benefit of the authors (and your $200 publishing discount) .

Structure and Criteria
Please read the 'Structure and Criteria' page for general guidance.

Raw data check
Review the raw data.

Image check
Check that figures and images have not been inappropriately manipulated.

Privacy reminder: If uploading an annotated PDF, remove identifiable information to remain anonymous.

Files
Download and review all files from the materials page.

10 Figure file(s)
2 Table file(s)
2 Other file(s)

Structure and Criteria

Structure your review

The review form is divided into 5 sections. Please consider these when composing your review:

1. **BASIC REPORTING**
2. **EXPERIMENTAL DESIGN**
3. **VALIDITY OF THE FINDINGS**
4. General comments
5. Confidential notes to the editor

You can also annotate this PDF and upload it as part of your review

When ready submit online.

Editorial Criteria

Use these criteria points to structure your review. The full detailed editorial criteria is on your guidance page.

BASIC REPORTING

- Clear, unambiguous, professional English language used throughout.
- Intro & background to show context. Literature well referenced & relevant.
- Structure conforms to PeerJ standards, discipline norm, or improved for clarity.
- Figures are relevant, high quality, well labelled & described.
- Raw data supplied (see PeerJ policy).

EXPERIMENTAL DESIGN

- Original primary research within Scope of the journal.
- Research question well defined, relevant & meaningful. It is stated how the research fills an identified knowledge gap.
- Rigorous investigation performed to a high technical & ethical standard.
- Methods described with sufficient detail & information to replicate.

VALIDITY OF THE FINDINGS

- Impact and novelty not assessed. Negative/inconclusive results accepted. *Meaningful* replication encouraged where rationale & benefit to literature is clearly stated.
- All underlying data have been provided; they are robust, statistically sound, & controlled.
- Speculation is welcome, but should be identified as such.
- Conclusions are well stated, linked to original research question & limited to supporting results.

Standout reviewing tips

The best reviewers use these techniques

Tip	*Example*
Support criticisms with evidence from the text or from other sources	*Smith et al (J of Methodology, 2005, V3, pp 123) have shown that the analysis you use in Lines 241-250 is not the most appropriate for this situation. Please explain why you used this method.*
Give specific suggestions on how to improve the manuscript	*Your introduction needs more detail. I suggest that you improve the description at lines 57- 86 to provide more justification for your study (specifically, you should expand upon the knowledge gap being filled).*
Comment on language and grammar issues	*The English language should be improved to ensure that an international audience can clearly understand your text. Some examples where the language could be improved include lines 23, 77, 121, 128 – the current phrasing makes comprehension difficult.*
Organize by importance of the issues, and number your points	*1. Your most important issue* *2. The next most important item* *3. …* *4. The least important points*
Please provide constructive criticism, and avoid personal opinions	*I thank you for providing the raw data, however your supplemental files need more descriptive metadata identifiers to be useful to future readers. Although your results are compelling, the data analysis should be improved in the following ways: AA, BB, CC*
Comment on strengths (as well as weaknesses) of the manuscript	*I commend the authors for their extensive data set, compiled over many years of detailed fieldwork. In addition, the manuscript is clearly written in professional, unambiguous language. If there is a weakness, it is in the statistical analysis (as I have noted above) which should be improved upon before Acceptance.*

Antibacterial activity and mechanism of sanguinarine against *Providencia rettgeri in vitro*

Qian Zhang [1, 2, 3, 4], **Miao Liu** [5], **Yansi Lyu** [1], **Jingkai Huang** [1], **Xinchen Li** [6], **Xiaodong Zhang** [1], **Na Yu** [1], **Ziping Wen** [1], **Si Chen** [Corresp., 3, 7], **Weidong Qian** [Corresp. 5]

[1] Department of Dermatology, Shenzhen University General Hospital, Shenzhen University, Shenzhen 518060, P. R. China., Shenzhen, China

[2] College of Physics and Optoelectronic Engineering, Shenzhen University, Shenzhen 518060, P. R. China., Shenzhen, China

[3] Shenzhen University Health Science Center, Shenzhen 518060, P. R. China, Shenzhen, China

[4] Department of Dermatology, PLAGH Hainan Hospital Of PLA General Hospital, Sanya 572013, P. R. China., Sanya, China

[5] School of Food and Biological Engineering, Shaanxi University of Science and Technology, Xi'an, 710021, P. R. Chian, Xi'an, China

[6] Shool of Food and Biological Engineering, Shaanxi University of Science and Technology, Xi'an, 710021, P. R. Chian, Xi'an, China

[7] Department of Immunology, Shenzhen University School of Medicine, Shenzhen 518037, P. R. China, Shenzhen, China

Corresponding Authors: Si Chen, Weidong Qian
Email address: chensi@szu.edu.cn, qianweidong@sust.edu.cn

Background Sanguinarine (SAG), a benzophenanthridine alkaloid, can be extracted from the rhizome of *Sanguinaria canadensis*. Studies found that SAG has antioxidant, anti-inflammatory, and antiproliferative activities in a number of malignancies and exhibits robust antibacterial activities. Little has been reported on the action of SAG against *Providencia rettgeri*. This study aimed to evaluate the antimicrobial and antibiofilm activities of SAG against *P. rettgeri in vitro*.

Methods The gradient diffusion method was used to determine the minimum inhibitory concentration (MIC) of SAG against *P. rettgeri.* The intracellular ATP concentration, intracellular pH (pH_{in}), and cell membrane integrity and potential were measured. Confocal laser scanning microscopy (CLSM), field emission scanning electron microscopy (FESEM), and crystal violet staining were used to measure the antibiofilm formation of SAG.

Results The results revealed that the MIC of SAG against *P. rettgeri* was 7.8 μg/mL. SAG inhibited the growth of *P. rettgeri* and destroyed the integrity of *P. rettgeri* cell membrane, as reflected mainly in the decrease in the intracellular ATP concentration, pH_{in}, and cell membrane potential and significant change in cellular morphology. The results of CLSM, FESEM, and crystal violet staining indicated that SAG exhibited strong inhibitory effects on the biofilm formation of *P. rettgeri* and led to the inactivity of biofilm-related *P. rettgeri* cells.

Conclusions These findings revealed the antibacterial potential of SAG, especially against *P. rettgeri*, and its potential as a SAG natural preservative to control *P. rettgeri*-related infections in the future.

Antibacterial activity and mechanism of sanguinarine against *Providencia rettgeri in vitro*

Qian Zhang[1,2,3,4], Miao Liu[5], Yansi Lyu[1], Jingkai Huang[1], Xin-chen Li[5], Xiaodong Zhang[1], Na Yu[1], Ziping Wen[1], Si Chen[3,6,*], Weidong Qian[5,*]

[1] Department of Dermatology, Shenzhen University General Hospital, Shenzhen University, Shenzhen 518060, P. R. China.
[2] College of Physics and Optoelectronic Engineering, Shenzhen University, Shenzhen 518060, P. R. China.
[3] Shenzhen University Health Science Center, Shenzhen 518060, P. R. China
[4] Department of Dermatology, PLAGH Hainan Hospital Of PLA General Hospital, Sanya 572013, P. R. China.
[5] School of Food and Biological Engineering, Shaanxi University of Science and Technology, Xi'an, 710021, P. R. China
[6] Department of Immunology, Shenzhen University Health Science Center, Shenzhen 518060, P. R. China

Corresponding Author:

Si Chen, Weidong Qian

3688 Nanhai Ave, Shenzhen, Guangdong, 518060, China; Weiyang road, Xi'an, Shaanxi, 710021, China.

Email address: chensi@szu.edu.cn (S.C); qianweidong@sust.edu.cn (W-d, Q)

Abstract

Background Sanguinarine (SAG), a benzophenanthridine alkaloid, can be extracted from the rhizome of *Sanguinaria canadensis*. Studies found that SAG has antioxidant, anti-inflammatory, and antiproliferative activities in a number of malignancies and exhibits robust antibacterial activities. Little has been reported on the action of SAG against *Providencia rettgeri*. This study aimed to evaluate the antimicrobial and antibiofilm activities of SAG against *P. rettgeri in vitro*.

Methods The gradient diffusion method was used to determine the minimum inhibitory concentration (MIC) of SAG against *P. rettgeri.* The intracellular ATP concentration,

intracellular pH (pHin), and cell membrane integrity and potential were measured. Confocal laser scanning microscopy (CLSM), field emission scanning electron microscopy (FESEM), and crystal violet staining were used to measure the antibiofilm formation of SAG.

Results The results revealed that the MIC of SAG against *P. rettgeri* was 7.8 μg/mL. SAG inhibited the growth of *P. rettgeri* and destroyed the integrity of *P. rettgeri* cell membrane, as reflected mainly in the decrease in the intracellular ATP concentration, pHin, and cell membrane potential and significant change in cellular morphology. The results of CLSM, FESEM, and crystal violet staining indicated that SAG exhibited strong inhibitory effects on the biofilm formation of *P. rettgeri* and led to the inactivity of biofilm-related *P. rettgeri* cells.

Conclusions These findings revealed the antibacterial potential of SAG, especially against *P. rettgeri*, and its potential as a SAG natural preservative to control *P. rettgeri*-related infections in the future.

Introduction

Providencia rettgeri is a common Gram-negative bacilli from the Enterobacteriaceae family and often isolated from wounds, the urinary tract, faces of reptiles, and blood of humans(Wie, 2015). *P. rettgeri* may cause gastroenteritis and bacteremia(Wie, 2015), which are thought to be the main causes of travelers' diarrhea (Yoh et al., 2005), and is considered a hospital pathogen that often causes urinary tract infections (Armbruster et al., 2014). The first infection of multidrug-resistant *P. rettgeri* in a neonate caused late-onset neonatal sepsis (Sharma et al., 2017), which was resistant to ampicillin, polymyxins, and first-generation cephalosporins (Magiorakos et al., 2012), and was challenging for the treatment of *P. rettgeri* infection. In recent years, *P. rettgeri* had been the focus of researchers due to the emergence of new strains (Mataseje et al., 2014)(Tada et al., 2014), which threatened public health globally. More importantly, at the beginning of the 21st century, *P. rettgeri* caused two food poisoning outbreaks, as reported by the Chinese Center for Disease Control (Murata et al., 2001). The report revealed that the risk of exposure to *P. rettgeri* extended beyond persons who traveled and were hospitalized and interacted with the general public.

Biofilms increase food safety risks by increasing the resistance of embedded bacteria to stresses often encountered in food processing and by acting as a persistent source of microbial contamination (Giaouris et al., 2014). Thus, another major reason *P. rettgeri* causes food contamination is the robustness of bacterial biofilms. Therefore, there is an urgent need to increase the supply of the ideal preservative against *P. rettgeri* in food, preferably an extract from plants, where safety is very important.

Sanguinarine [13-methyl(1,3)benzodioxolo(5,6-c)-1,3-dioxolo(4,5)phenanthridinium] (SAG) is an isoquinoline derivative and belongs to benzophenanthridines. The molecular formula is $C_2H_{15}NO_5$(Yatoo et al., 2018). SAG is extracted from the rhizome of *Sanguinaria canadensis*. Previous studies revealed that *Sanguinaria* has antimicrobial, antioxidant, and anti-inflammatory abilities (Firatli et al., 1994), which are cytotoxic and cytostatic on many human cancer cells through its action on the Na^+/K^+-ATPase transmembrane protein. It is known that Na^+/K^+-ATPase with normal physiological functions maintains the resting potential and regulates the cellular volume by pumping sodium out of cells and potassium into cells, both against their concentration gradients (Singh and Sharma, 2018). New studies reported that *Sanguinaria* possesses antimicrobial acidity against *Psoroptes cuniculi*(Miao et al., 2012).

Although *Sanguinaria* has been verified against some bacteria, its effect on *P. rettgeri* has not been reported. Therefore, this study aimed to investigate the antimicrobial and antibiofilm activities of *Sanguinaria* against *P. rettgeri.*

Materials and Methods

Reagents

Sanguinaria was purchased from Nanjing Zelang Meditech Ltd., with a purity level of 98%. For all experiments, 10 mg/mL SAG in dimethyl sulfoxide (DMSO; Sigma-Aldrich) was used as stock, and a tenfold dilution of the stock was made in DMSO before addition to culture suspensions to obtain the required SAG concentrations.

Bacterial and culture condition

P. rettgeri can form normal biofilms. Clinical *P. rettgeri* strains used in this study included *P. rettgeri*-1, *P. rettgeri*-2, *P. rettgeri*-3, and *P. rettgeri*-4, *P. rettgeri*-5, *P. rettgeri*-6, *P. rettgeri*-7 the seven *P. rettgeri* isolates originally derived from the hydrothorax and urine of patients. The strains were routinely grown in tryptic soy broth (TSB) at 37°C in a shaking incubator. The cells were standardized according to 0.5 McFarland standards to create inoculum densities of 2×10^6 colony-forming units (CFU)/mL for use in antibacterial activity determination assay and bacterial broth cultures of 5×10^8 CFU/mL for biofilm assays.

Minimum inhibitory concentration (MIC) test

The MIC test was conducted according to the standard susceptibility broth dilution technique with minor modifications (Choi et al., 2017). The *P. rettgeri* culture was diluted into 96-well plate (Costar, Corning, NY, USA) using TSB at 10^2 CFU/mL. SAG was prepared at final concentrations of 0, 7.8, 15.6, 31.25, 62.5, 125, 250, and 500 μg/mL and then incubated at 37°C for 24 h. The growth was surveyed for turbidity in microwells. MIC was defined as the minimum SAG concentration that completely inhibited the growth of visible bacteria. All experiments were repeated at least thrice.

Growth curves

The method of Xu et al. for establishing growth curves (Xu et al., 2017) was modified slightly to assess the antimicrobial effect of SAG on *P. rettgeri*. Then, 100-fold dilution log-phase bacterial suspension (100 μL; OD_{600} = 0.5) into TSB containing SAG at final concentrations of 0, 1:8, 1:4, 1:2, 1, and 2 MIC was incubated at 37°C with gentle shaking at 150 rpm. An aliquot of the culture was removed at 1 h intervals of different times of growth, which was plated on tryptic soy agar after adequate serial dilutions. Finally, the well plates were incubated at 37°C for 24 h, and the colonies were counted manually. The dynamic growth or inactivation curves for each treatment were constructed based on the viable cell counts.

Measurement of ATP levels

The method of Sianglum et al. (Sianglum et al., 2018) was used to determine the intracellular ATP concentration of *P. rettgeri* with minor modifications. Exponential-phase *P. rettgeri* at 1×10^5 CFU/mL was treated with 0, 1, and 2 MIC of SAG at 37°C for 1, 2, and 3 h, respectively, to evaluate the amount of intracellular ATP and release of ATP, and the cells were harvested by centrifugation (8000 ×g, 10 min). In parallel, the supernatant was filtered, degermed, and transferred to a new test tube to measure the extracellular ATP, which leaks from the bacterial cells. The bacterial precipitate was washed twice with 1 mM phosphate-buffered saline (PBS; pH 7.0), suspended in the same PBS, and then placed on ice. Intracellular ATP was extracted by DMSO. ATP was measured using the ATP Assay Kit according to the manufacturer's instructions (Beyotime Bioengineering Institute, Shanghai, China).

Intracellular pH (pH_{in}) test

The modified method of Shi et al. was used to evaluate pH_{in}(Shi et al., 2016). Overnight cultures of 300 μL were transferred to 30 mL TSB and then incubated at 37°C for 8 h. After harvesting, the cells were centrifuged (8000 ×g, 10 min), washed twice with 50 mM HEPES and 5 mM EDTA (mixed solution at pH 8.0), and then resuspended in 20 mL mixed solution. Subsequently, 3 μM carboxyfluorescein diacetate succinimidyl ester (CFDA-

SE; Beyotime Bioengineering Institute) was added. The mixture was incubated at 37°C for 20 min, then washed once with the mixture solution (pH 7.0; 50 mM PBS and 10 mM $MgCl_2$), and resuspended in the same buffer. Glucose (10 mM final concentration) was added to eliminate nonconjugated CFDA-SE, the mixture was incubated at 37°C for 30 min and washed twice, and the cells were resuspended with 50 mM potassium phosphate buffer (pH 7.0) and stored in ice.

Fluorescently labeled cell suspensions were treated with three different concentrations (0, 1, and 2 MIC) of SAG and then transferred evenly into a black opaque 96-well flat-bottomed plate (Nunc, Copenhagen, Denmark). After exposure for 20 min, fluorescence intensity was tested under two excitation wavelengths of 440 and 490 nm, and the emission wavelength was collected at 520 nm, where the excitation slit width was 9 nm and the emission was 20 nm. pH_{in} was tested as the ratio of the fluorescence signal at the pH-sensitive wavelength of 490 nm to the fluorescence signal at the pH-insensitive wavelength of 440 nm. In the study, all measurements were performed on a microplate reader (Thermo Fisher Scientific, Finland). During the monitoring period, the system was maintained at 25°C, and the fluorescence of the acellular control group was measured and subtracted from the value of the treated suspension.

The calibration curves were built for CFDA-SE-loaded cells with mixed solutions of different pH values. The mixture consisted of glycine (50 mM), citric acid (50 mM), $Na_2HPO_4{\cdot}2H_2O$ (50 mM), and KCl (50 mM). The pH was adjusted to various values (2–10) with NaOH or HCl, and valinomycin (10 μM) and nigrosine (10 μM) were added to adjust pH_{in} and pH_{out}. Finally, fluorescence intensity was evaluated at 25°C.

Determination of membrane potential

The method of Wang et al. was used to determine the membrane potential with minor modifications (Wang et al., 2018). The changes in bacterial membrane potential were used to determine the fluorescent probe bis-(1,3-dibutylbarbituric acid) trimethine oxonol [$DiBAC_4(3)$]. Bacterial cells were harvested in log-phase growth, centrifuged at 4000 × g for 10 min, and washed twice with 10 mM PBS (pH 7.0), adjusting the bacterial concentration to 1×10^5 CFU/mL, and treated with three different SAG concentrations (0, 1, and 2 MIC) to the bacterial suspensions at 37°C for 2 h, incubated with $DiBAC_4(3)$ at 25°C for 10 min in the dark, and then washed with PBS once. The microplate reader calculated the florescence at excitation/emission wavelengths of 492/515 nm. The excitation and emission slit widths were 3 and 5 nm, respectively.

Evaluation of bacterial membrane integrity

The modified method of Liu et al. (Liu et al., 2018) was applied to assess the cell membrane integrity of *P. rettgeri* cells using confocal laser scanning microscopy (CLSM; Zeiss LSM 880 with Airyscan, Bonn, Germany).

Mid-log-phase cells were treated with three different SAG concentrations (0, 1, and 2 MIC) for 2 h, harvested by centrifugation at 8000 ×g for 5 min, and then resuspended with 0.01 M PBS of equivalent volume. After incubation with the mixed solution of SYTO9 and propidium iodide (PI) at 25°C for 15 min, cells were finally collected and washed with 10 mM PBS to remove excess dyes.

Transmission electron microscopy (TEM)

Transmission electron microscopy (TEM) (G2 F20 S-Twin; FEI, Hillsboro, OR, USA) observation was performed according to Joung et al.(Joung et al., 2016). with some modification. Exponential-phase *P. rettgeri* cultures were prepared for overnight cultures and incubated at 37°C in TSB until they reached mid-log-phase growth. The cell suspension was treated with three different SAG concentrations (0, 1, and 2 MIC) for another 4 h at 37°C, centrifuged (10,000 × g, 8 min), and washed twice with 0.85% NaCl. Subsequently, the suspension was removed, cell pellets were fixed with 2.5% glutaraldehyde for 12 h at 37°C, and different concentrations of alcohol (20%, 50%, 70%, 80%, 90%, and 100%) were used for dehydration for 15 min and embedded in resin. Ultrathin samples were incised by ultra-microtome, and uranyl acetate stain was used for TEM.

Field emission scanning electron microscopy (FESEM)

After treatment with SAG at different concentrations, the morphology of bacteria had some changes, as observed by FESEM (Nova Nano SEM-450; FEI, Eindhoven, Netherlands) as described previously(Shi et al., 2018). The log-phase cells were treated with three different concentrations (0, 1, and 2 MIC) of SAG for 4 h at 37°C, washed with 0.01 M PBS (pH 7.0), and fixed in 2.5% glutaraldehyde for 12 h at 4°C. The cells were dehydrated by sequential treatment with ethanol concentrations ranging from 30% to 100% for 10 min. Finally, the cells were fixed to the FESEM scaffold, gold sputtering was used to coat the cells under vacuum conditions, and FESEM was used to examine cell morphology.

Inhibition of the biofilm formation

The effect of SAG on the biofilm formation of *P. rettgeri* was examined quantitatively in 96-well plates by the modified crystal violet staining method, as described by Weidong Qian et al. (19). *P. rettgeri* cells were incubated in the presence of SAG at 0, 1:32, 1:16, 1:8, 1:4, 1:2, 1, and 2 MIC for 24 h and washed thrice with sterile distilled water to remove the planktonic cells and loose adherent cells in the plate, and the biofilm of cells was stained with 1% crystal violet (100 μL), incubated for 15 min at 28°C, and washed thrice with sterile distilled water. Crystal violet, which bound to the biofilm, was extracted with 30% acetic acid and transferred to a new plate of the aliquot

from each well. Then, absorbance was tested at 570 nm. The specific biofilm formation index was determined by attaching stained bacteria (OD570) normalized with the cell growth (OD630).

The effects of SAG on the biofilm formation were visually observed by FESEM and CLSM as described (19). The slides of the cells were treated with different concentrations at 0, 1:16, 1:8, and 1:4 MIC incubated for 24 h at 37°C, washed thrice with 0.85% NaCl, fixed with 2.5% glutaraldehyde in 200 mM phosphate buffer for 4 h at 25°C, dehydrated with different concentrations of ethanol gradient (30%, 60%, 70%, 80%, 90%, and 100%) for 20 min for each concentration, and treated with gold spray. The biofilm formation of *P. rettgeri* was visually observed by FESEM, with one point selected for each slide.

P. rettgeri cells, which grew on the slides for 12 h, were treated with different concentrations (0, 1:16, 1:8, and 1:4 MIC) for culture for 24 h and then washed thrice with 0.85% NaCl. *P. rettgeri* cells grown on the slides were treated with CFDA-SE and then incubated for 15 min at 25°C for direct visual observation of the biofilm formation, which was tested by CLSM. The fluorescence intensity of the cells was measured at excitation/emission wavelengths of 488/542 nm for CFDA-SE.

Biofilm matrix by CLSM

The changes in major biofilm matrix levels within 24-h-old biofilms of mono or dual species in the presence of SAG were detected by CLSM of the biofilm matrix combined with different dyes. Briefly, biofilms were prepared using the procedure described in the crystal violet biofilm assay section. The resulting samples were washed thrice with sterile 1 mM PBS (pH 7.4) and labeled respectively with three fluorescent dyes: (1) 25% (v/v) SYPRO Ruby, which stains most classes of proteins and 2 μM SYTO9 dye; (2) 5 μg/mL WGA dye, which labels polysaccharides and 5 μg/mL water-soluble FM® dyes; and (III) 2 μM PI dye and 2 μM SYTO9 dye. Subsequently, the biofilm was washed twice with 1 mM PBS to remove all planktonic bacteria, where the excitation/emission wavelengths were 450/610 nm for SYPRO Ruby (red), 498/517 nm for SYTO9 (green), 488/617 nm for PI (red), 495/519 nm for WGA (green), and 479/565 nm for water-soluble FM® dyes (red). Color confocal images were observed by CLSM.

Diffusion bioassay for gatifloxacin within biofilms

To evaluate the diffusion of antibiotics into biofilms, the diffusion of gatifloxacin into biofilms was identified based on the intrinsic fluorescence of CLSM. The biofilms described above were placed on glass coverslips inside the 24-well plate for 48 h at 37°C in the presence of LUT at 0, 1:16, 1:8, and 1:4 MIC, withdrawn and gently washed thrice with 10 mM PBS, and added with gatifloxacin at a final concentration of 0.4 mg/mL and further incubated at 37°C for 4 h. Then, 3 μM SYTO 9 was added and incubated for 15 min to observe gatifloxacin diffusion within biofilms. The samples were washed with 10 mM PBS thrice and observed by CLSM. The emission

peak of gatifloxacin at 495 nm was recorded upon excitation at 291 nm. At least three random fields were visualized for each biofilm, and representative images were displayed.

Statistical analysis

All experiments in this study were conducted thrice independently. Each biological replicate was needed to carry out two technical replicates. Data were expressed as mean ± standard deviation (SD). $P < 0.05$ was considered statistically significant. Results were analyzed using Origin 8.5 statistics.

Results

MIC of SAG against *P. rettgeri*

According to the MIC in Table 1, *P. rettgeri* in this study manifested antibiotic resistance, as evidenced by MIC of ampicillin (32 μg/mL), cefepime (16–64 μg/mL), ertapenem (8 μg/mL), imipenem (16 μg/mL), tobramycin (8–16 μg/mL), amikacin (2–64 μg/mL), piperacillin/tazobactam (64–128 μg/mL), and nitrofurantoin (32–512 μg/mL) (Table 1). The results of the antibacterial activities of LUT are presented in Table 1. SAG inhibited the growth of *P. rettgeri* and exhibited robust antibacterial activity against *P. rettgeri*. SAG was effective with an MIC of 31.25, 15.6, and 7.8 μg/mL against *P. rettgeri*. Here, *P. rettgeri*-4 was employed for further experiments to ensure that the results were repeatable.

Effects of SAG on the growth kinetics of *P. rettgeri* cells

The biomass of *P. rettgeri* was decreased when treated with SAG at MIC in media (Figure 1); however, cells treated with SAG at 2 MIC exhibited a significant decline in the number of living cells, which was lower than the detection limit after 24 h. In contrast, at concentrations of 1:8 and 1:4 MIC, the growth curves exhibited weaker increases and lower growth rates. Comparing this with different growth curves, higher SAG concentrations resulted in a sharp reduction in the relative number of living cells compared with lower SAG concentrations.

SAG treatment led to a decrease in the intracellular ATP concentrations, pH, and membrane potential of *P. rettgeri*

When *P. rettgeri* cells were treated with SAG at 1 and 2 MIC, the intracellular ATP concentration was significantly decreased ($p < 0.05$) compared with the untreated control group in Figure 2A; however, there were no significant differences between the cells treated with SAG at 1 and 2 MIC, but the decrease in ATP levels was positively followed by the increase in the SAG concentration. At the same time, the extracellular ATP concentration of *P. rettgeri* increased in a concentration-dependent manner, and its action was time dependent (Figure 2B).

The pH_{in} of *P. rettgeri* after SAG treatment significantly changed, as presented in Figure 2C. In this study, the original pH_{in} of *P. rettgeri* was 5.97 ± 0.25. Treatment with SAG at 1 MIC led to a significant ($P < 0.01$) decrease in pH_{in} of *P. rettgeri* from 5.97 ± 0.25 to 4.53 ± 0.25, whereas with SAG at 2 MIC, the pH_{in} of *P. rettgeri* was reduced from 5.97 ± 0.25 to 3.47 ± 0.25 ($P < 0.01$).

Fluorescence intensity was used to measure the membrane potential. In Figure 2D, the fluorescence intensities of *P. rettgeri* were exposed to SAG at 1 MIC for 2 h, which were less than those of the unexposed control group. Equivalently, when the SAG concentration increased from 1 to 2 MIC, the membrane potential decreased significantly ($P < 0.01$).

SAG treatment increased the cell membrane permeability of *P. rettgeri*

The cells with intact membrane stained with CFDA-SE generated bright green fluorescence, but membrane-damaged cells loaded with PI exhibited red fluorescence. In Figure 3, *P. rettgeri* cells of the untreated control group generated bright green fluorescence, which revealed the physical integrity of the cell membrane. In contrast, the cells treated with 1 MIC of SAG exhibited significantly reduced green fluorescence and increased red fluorescence. With the addition of SAG concentration, green fluorescence intensity disappeared, and red fluorescence intensity increased significantly.

Treatment with SAG led to changes in the cell morphology of *P. rettgeri*

In this study, TEM was used to assess the level of cell wall damage and intracellular modification in SAG-treated *P. rettgeri.* The untreated *P. rettgeri* cells exhibited a visible outline and the peptidoglycan layer (Figure 4A), but *P. rettgeri* cells treated with SAG at 1 MIC were malformed, damaged, and out of proportion (Figure 4B). In contrast, *P. rettgeri* cells treated with SAG at 2 MIC exhibited a wavy contour of the cytoplasmic membrane and exhibited dense, undifferentiable cellular content, indicating a significant shrinkage of the cytoplasm (Figure 4C). Consequently, SAG-treated *P. rettgeri* could damage the cell membrane and cell wall outline.

The cell morphology after treatment with SAG presented significant changes using FESEM. Compared with the normal smooth cell surface of the untreated group (Figure 5A), cells treated with SAG at 1 MIC exhibited significant enlargement, uneven size, and rough surface (Figure 5B). In addition, cells treated with SAG at 2 MIC presented significant surface collapse and expansion on the cell membrane due to the cell wall destruction (Figure

5C), which indicated a positive correlation between the increase in SAG concentration and the degree of cell membrane damage.

Inhibitory effect of SAG on the biofilm formation of *P. rettgeri*

In the study, the crystal violet staining method was used to assess the effect of SAG on the inhibitory effects of biofilm growth of *P. rettgeri* by FESEM and CLSM. As presented in Figure 6, SAG presented a statistically significant inhibitory effect on the biofilm formation of *P. rettgeri* at different concentrations ($P < 0.05$). The biofilm formation index of the untreated control group was approximately 3.6. The biofilm formation was inhibited by 68% when treated with 1:16 MIC of SAG; when the SAG concentration was higher than 1:4 MIC, the biofilm could be inhibited by more than 95%.

In addition, a significant inhibition of the biofilm formation at 1:16, 1:8, and 1:4 MIC was observed in SAG treatment compared with the untreated group by FESEM and CLSM (Figure 7). In contrast, SAG treatment at 1:4 MIC significantly inhibited the majority of biofilms, suggesting that SAG has a strong ability to inhibit the biofilm formation of *P. rettgeri*.

Inactivation effect of SAG on the biofilm of *P.rettgeri* cells

The inactivation effect of SAG against 36-h-old biofilm-associated *P. rettgeri* cells is presented in Figure 8. The untreated group was almost entirely green, as observed by CLSM (Figure 8A and E), indicating that most of the cell membranes of *P. rettgeri* cells embedded in biofilms were integrated and viable. In contrast, *P. rettgeri* cells within biofilm were treated with SAG at 16 MIC, and CLSM observed numerous bright red, revealing that most of the bacterial cell membranes within biofilms were impaired, as presented in Figure 8D and H. Further, the SAG concentration was increased from 4 to 8 MIC, and the green signal on the membrane gradually disappeared and the red signal gradually increased (Figure 8B, C, F, and G), indicating that intact and viable biofilms changed with the increase in concentration. These results suggested that SAG can osmose biofilms by *P. rettgeri* and lead to the inactivation of *P. rettgeri* cells within biofilms.

SAG could change the biofilm matrix composition of *P. rettgeri* cells

The biofilm matrix commonly comprises proteins, nucleic acid (eDNA), and carbohydrates, which provide structural rigidity and protection from the external environment to control gene regulation and nutrient adsorption (Hobley et al., 2015). Thus, the change in the composition of the biofilm matrix could affect the biofilm formation. Therefore, the influence of SAG on proteins, nucleic acid (eDNA), and carbohydrates of *P. rettgeri* was investigated. The changes in major biofilm matrix levels within 24-h-old biofilms of mono or dual species in the

presence of SAG were detected by CLSM in Figure 9. Different reagents were used to mark the eDNA and proteins red and the carbohydrates green. The untreated groups of nucleic acids and proteins were almost red, as observed by CLSM; with the increase in SAG concentration, the red signal was gradually reduced (Figure 9A and C). The untreated group of carbohydrates was green, as observed by CLSM, and with the increase in SAG concentration, the green signal gradually disappeared (Figure 9B), indicating that nucleic acid, protein, and carbohydrate contents decrease with the increase in SAG concentration.

Effect of SAG on biofilms of diffusion

Gatifloxacin was used to verify the effect of SAG on biofilm diffusion, which was monitored using fluorescence CSLM. *P. rettgeri* biofilms were grown with different SAG concentrations for 48 h and then added with gatifloxacin for 4 h. Formed biofilms were stained with SYTO9 to allow the visualization of nucleic acid (green fluorescence).

Gatifloxacin significantly diffused in the 0 MIC group (Figure 10A). In contrast, in mixed biofilms with 1:4 MIC of SAG, the gatifloxacin signal was minimally detected (Figure 10D). As the SAG concentration increased, the signal diffusion became weaker, which proved that SAG inhibited the biofilm formation.

Discussion

This is the first study that evaluated the antibacterial activity and action mode of SAG against *P. rettgeri*. As observed by TEM, CLSM, and FESEM, the results revealed a significant effect of SAG against *P. rettgeri* biofilms, including inhibitory effect on biofilm substance expression and formation and biofilm inactivation. It was also found that SAG could decrease intracellular ATP and change in pH_{in} and reduce the membrane potential.

SAG had a strong activity against *P. rettgeri* biofilms. What's more, SAG did not only inhibit the biofilm formation but also destroyed the intact and viable biofilm. At 1:16 MIC, SAG inhibited biofilm formation by approximately 68%, whereas at 1:4 MIC, more than 95% of the biofilm was inhibited; thus, an outstanding antifungal effect of SAG was observed on *P. rettgeri.*

ATP depletion is a common biological change associated with cell damage, suggesting that ATP can be used as a potential indicator of the effects of antimicrobial agents on the intact and viable cell membrane. These results presented that SAG-treated *P. rettgeri* exhibited a remarkable decrease in intracellular ATP, and changes in intracellular and extracellular ATP balance in *P. rettgeri* cells were observed, suggesting damage of the cell membrane. These results were consistent with those of a previous report. A similar study found that vanillic acid

induced a significant decrease in intracellular ATP concentration of carbapenem-resistant *Enterobacter cloacae*, as reported by Qian et al. (Qian et al., 2019). Kang et al.(Kang et al., 2019). verified that a significant increase in extracellular ATP concentration was found in *Staphylococcus aureus* cells exposed to peppermint essential oil.

pH_{in} has a critical influence on cell physiology, including DNA replication, RNA transcription, protein synthesis, and enzyme activity. Moreover, pH_{in} is positively related to intact and viable cell membrane (Gonelimali et al., 2018). Consequently, the change in pH_{in} could suggest damage of the cell membrane. In this study, the change in pH_{in} of *P. rettgeri* was significantly related to SAG concentration, in which the addition of 2 MIC of SAG led to the reduction of the pH_{in} from 5.97 ± 0.25 to 3.47 ± 0.25. A similar study by Sanchez et al. (Sánchez et al., 2010) reported that treatment of *Vibrio cholerae* strain with all plant extracts significantly decreased the pH_{in} from 7.2 to 3.9 ± 0.5 ($P < 0.05$). Faraja et al.(Gonelimali et al., 2018) also found that the decrease in pH_{in} was tested in *S. aureus* and *Escherichia coli* cells after exposure to plant extracts. Hence, as described in previous literature for plant-derived products, the effect of SAG on *P. rettgeri* could be cleared as the breaking to intact and viable cell membrane. Additionally, when SAG entered into cells, it could cause hyperpolarization across the cell membrane, thus making the internal membrane potential more negative. Compared with the untreated control group, when the SAG concentration increased from 1 to 2 MIC, the membrane potential significantly decreased. Similarly, Hua Zhong et al.(Zhong et al., 2017) reported that SAG could decrease the membrane potential of *Candida albicans* cells. These results suggested that SAG caused plasma membrane hyperpolarization for determined bacteria, which possibly led to the disruption of cell metabolic activity and cell death.

Previous studies also indicated that *P. rettgeri* cells experienced significant membrane dissolution, as observed by CLSM, whereas leakage of cytoplasmic components was found after exposure to SAG by TEM. CLSM revealed that permeability of cell membrane increased after treatment with SAG. The 2 MIC-exposed *P. rettgeri* cells were apparently entirely red, indicating that cell membranes were mostly destroyed, and some substances could move allodially in and out of the cell. Therefore, FESEM images of *P. rettgeri* cells exposed to SAG at 2 MIC revealed that the cells had severe morphological alterations, and MIC-exposed cells were visibly extended and had a rough surface. The physical and morphological changes in *P. rettgeri* cells may be due to the effect of SAG on membrane permeability and integrity. In contrast, dense, undifferentiated intracellular materials in SAG-exposed cells were observed by TEM. Also, CLSM revealed that almost all bacterial cells were damaged after exposure to SAG at 2 MIC. As reported by Matijasevic et al.(Danka et al., 2016), FESEM and TEM were used to observe the morphological changes of *S. aureus* cells treated with *Coriolus versicolor* methanol extract.

Previous studies verified that biofilms could enhance bacterial resistance to adverse environmental pressures, including resistance to antibiotics and antimicrobial agents(Tim et al., 2017). Exopolysaccharides, proteins, and extracellular DNA formed bacterial cells in biofilms, which were embedded in extracellular polymeric substances. In this study, the effect of SAG on biofilm formation and biofilm-associated cell inactivation was further illustrated, and the results of crystal violet staining revealed that SAG at different concentrations presented inhibitory effects on the biofilm formation of *P. rettgeri*. Moreover, FESEM and CLSM observed that SAG-exposed cells exhibited substantially decreased adhesion and survival, revealing that biofilm formation was significantly inhibited by SAG.

These results are consistent with the observation of Benjamin et al.(Bhunu et al., 2017) that demonstrated the inhibitory effects of *Parinari curatellifolia* leaf extracts on biofilm formation. In addition, CLSM further exhibited that SAG presented robust impaired effects on biofilm-associated *P. rettgeri* cells. CLSM images of *P. rettgeri* cells within biofilms exposed to 4 MIC of SAG displayed dark red, proving that most of the cell membranes of cells in biofilm were damaged. These results were in agreement with the effectiveness of antistaphylococcal lysin CF-301 on the inactivation of 95 *S. aureus* strains within biofilms, as described by Raymond et al.(Schuch et al., 2017).

Conclusions

In our study, we confirmed that SAG was effective in inactivating both *P. rettgeri* cells, biofilm formation and integrity. SAG could induce cell lysis, and leading to cell membrane damage and leakage of intracellular components in *P. rettgeri* cells. In addition, 2MIC SAG could inactivate biofilm P.R cells, so it could be used as a natural antibacterial agent to control *P. rettgeri* pollution in the food industry.

Acknowledgements

This work was supported by the National Natural Science Foundation of China (No. 81902067 and 81300028).

References

Armbruster, C.E., Smith, S.N., Yep, A., Mobley, H.L.T., 2014. Increased incidence of urolithiasis and bacteremia during Proteus mirabilis and Providencia stuartii coinfection due to synergistic induction of urease activity. J. Infect. Dis. 209, 1524–1532.

Bhunu, B., Mautsa, R., Mukanganyama, S., 2017. Inhibition of biofilm formation in

Mycobacterium smegmatis by Parinari curatellifolia leaf extracts. BMC Complement Altern Med 17, 285.

Choi, H.-A., Cheong, D.-E., Lim, H.-D., Kim, W.-H., Ham, M.-H., Oh, M.-H., Wu, Y., Shin, H.-J., Kim, G.-J., 2017. Antimicrobial and Anti-Biofilm Activities of the Methanol Extracts of Medicinal Plants against Dental Pathogens Streptococcus mutans and Candida albicans. J. Microbiol. Biotechnol. 27, 1242–1248.

Danka, M., Panti? Milena, Ra?kovi? Bo?idar, Pavlovi? Vladimir, Duvnjak Dunja, Sknepnek Aleksandra, Nik?i? Miomir, 2016. The Antibacterial Activity of Coriolus versicolor Methanol Extract and Its Effect on Ultrastructural Changes of Staphylococcus aureus and Salmonella Enteritidis. Frontiers in Microbiology 7.

Firatli, E., Unal, T., Onan, U., Sandalli, P., 1994. Antioxidative activities of some chemotherapeutics. A possible mechanism in reducing gingival inflammation. J. Clin. Periodontol. 21, 680–683.

Giaouris, E., Heir, E., Hébraud, M., Chorianopoulos, N., Langsrud, S., Møretrø, T., Habimana, O., Desvaux, M., Renier, S., Nychas, G.-J., 2014. Attachment and biofilm formation by foodborne bacteria in meat processing environments: causes, implications, role of bacterial interactions and control by alternative novel methods. Meat Sci. 97, 298–309.

Gonelimali, F.D., Lin, J., Miao, W., Xuan, J., Charles, F., Chen, M., Hatab, S.R., 2018. Antimicrobial Properties and Mechanism of Action of Some Plant Extracts Against Food Pathogens and Spoilage Microorganisms. Front Microbiol 9, 1639.

Hobley, L., Harkins, C., MacPhee, C.E., Stanley-Wall, N.R., 2015. Giving structure to the biofilm matrix: an overview of individual strategies and emerging common themes. FEMS Microbiol. Rev. 39, 649–669.

435 Joung, D., Mun, S., Choi, S., Kang, O., Kim, S., Lee, Y., Zhou, T., Kong, R., Choi, J., Shin, D.,
436 2016. Antibacterial activity of oxyresveratrol against methicillin?resistant Staphylococcus aureus
437 and its mechanism. Experimental & Therapeutic Medicine.
438
439 Kang, J., Jin, W., Wang, J., Sun, Y., Wu, X., Liu, L., 2019. Antibacterial and anti-biofilm
440 activities of peppermint essential oil against Staphylococcus aureus. Lebensmittel-Wissenschaft
441 und-Technologie / Food Science and Technology.
442
443 Liu, F., Wang, F., Du, L., Zhao, T., Doyle, M.P., Wang, D., Zhang, X., Sun, Z., Xu, W., 2018.
444 Antibacterial and antibiofilm activity of phenyllactic acid against Enterobacter cloacae. Food
445 Control 84, 442–448.
446
447 Magiorakos, A.-P., Srinivasan, A., Carey, R.B., Carmeli, Y., Falagas, M.E., Giske, C.G.,
448 Harbarth, S., Hindler, J.F., Kahlmeter, G., Olsson-Liljequist, B., Paterson, D.L., Rice, L.B.,
449 Stelling, J., Struelens, M.J., Vatopoulos, A., Weber, J.T., Monnet, D.L., 2012. Multidrug-
450 resistant, extensively drug-resistant and pandrug-resistant bacteria: an international expert
451 proposal for interim standard definitions for acquired resistance. Clin. Microbiol. Infect. 18,
452 268–281.
453
454 Mataseje, L.F., Boyd, D.A., Lefebvre, B., Bryce, E., Embree, J., Gravel, D., Katz, K., Kibsey, P.,
455 Kuhn, M., Langley, J., Mitchell, R., Roscoe, D., Simor, A., Taylor, G., Thomas, E., Turgeon, N.,
456 Mulvey, M.R., Canadian Nosocomial Infection Surveillance Program, 2014. Complete
457 sequences of a novel blaNDM-1-harbouring plasmid from Providencia rettgeri and an FII-type
458 plasmid from Klebsiella pneumoniae identified in Canada. J. Antimicrob. Chemother. 69, 637–
459 642.
460
461 Miao, F., Yang, X.-J., Ma, Y.-N., Zheng, F., Song, X.-P., Zhou, L., 2012. Structural modification
462 of sanguinarine and chelerythrine and their in vitro acaricidal activity against Psoroptes cuniculi.
463 Chem. Pharm. Bull. 60, 1508–1513.
464

Murata, T., Iida, T., Shiomi, Y., Tagomori, K., Akeda, Y., Yanagihara, I., Mushiake, S., Ishiguro, F., Honda, T., 2001. A Large Outbreak of Foodborne Infection Attributed to\\r Providencia alcalifaciens. Journal of Infectious Diseases 184, 1050–1055.

Qian, W., Fu, Y., Liu, M., Wang, T., Zhang, J., Yang, M., Sun, Z., Li, X., Li, Y., 2019. In Vitro Antibacterial Activity and Mechanism of Vanillic Acid against Carbapenem-Resistant Enterobacter cloacae. Antibiotics (Basel) 8.

Sánchez, E., García, S., Heredia, N., 2010. Extracts of Edible and Medicinal Plants Damage Membranes of Vibrio cholerae. 《Applied & Environmental Microbiology》 76, 6888–6894.

Schuch, R., Khan, B.K., Raz, A., Rotolo, J.A., Wittekind, M., 2017. Bacteriophage Lysin CF-301, a Potent Antistaphylococcal Biofilm Agent. Antimicrob. Agents Chemother. 61.

Sharma, D., Sharma, P., Soni, P., 2017. First case report of Providencia Rettgeri neonatal sepsis. BMC Res Notes 10.

Shi, C., Che M, Zhang X, Liu Z, Meng R, Bu X, Ye H, Guo N, 2018. Antibacterial activity and mode of action of totarol against Staphylococcus aureus in carrot juice. Journal of Food Science & Technology 55, 924.

Shi, C., Zhang, X., Sun, Y., Yang, M., Song, K., Zheng, Z., Chen, Y., Liu, X., Jia, Z., Dong, R., Cui, L., Xia, X., 2016. Antimicrobial Activity of Ferulic Acid Against Cronobacter sakazakii and Possible Mechanism of Action. Foodborne Pathog. Dis. 13, 196–204.

Sianglum, W., Saeloh, D., Tongtawe, P., Wootipoom, N., Indrawattana, N., Voravuthikunchai, S.P., 2018. Early Effects of Rhodomyrtone on Membrane Integrity in Methicillin-Resistant Staphylococcus aureus. Microb. Drug Resist. 24, 882–889.

Singh, N., Sharma, B., 2018. Toxicological Effects of Berberine and Sanguinarine. Front Mol Biosci 5.

Tada, T., Miyoshi-Akiyama, T., Dahal, R.K., Sah, M.K., Ohara, H., Shimada, K., Kirikae, T., Pokhrel, B.M., 2014. NDM-1 Metallo-β-Lactamase and ArmA 16S rRNA methylase producing Providencia rettgeri clinical isolates in Nepal. BMC Infect. Dis. 14, 56.

Tim, J., Tolker-Nielsen Tim, Givskov Michael, 2017. Bacterial Biofilm Control by Perturbation of Bacterial Signaling Processes. International Journal of Molecular Sciences 18, 1970-1978.

Wang, Jianyu, Ma, M., Yang, J., Chen, L., Yu, P., Wang, Jun, Gong, D., Deng, S., Wen, X., Zeng, Z., 2018. In Vitro Antibacterial Activity and Mechanism of Monocaprylin against Escherichia coli and Staphylococcus aureus. J. Food Prot. 81, 1988–1996.

Wie, S.-H., 2015. Clinical significance of Providencia bacteremia or bacteriuria. Korean J. Intern. Med. 30, 167–169.

Xu, Y., Shi, C., Wu, Q., Zheng, Z., Liu, P., Li, G., Peng, X., Xia, X., 2017. Antimicrobial Activity of Punicalagin Against Staphylococcus aureus and Its Effect on Biofilm Formation. Foodborne Pathog. Dis. 14, 282–287.

Yatoo, M.I., Gopalakrishnan, A., Saxena, A., Parray, O.R., Tufani, N.A., Chakraborty, S., Tiwari, R., Dhama, K., Iqbal, H.M.N., 2018. Anti-Inflammatory Drugs and Herbs with Special Emphasis on Herbal Medicines for Countering Inflammatory Diseases and Disorders - A Review. Recent Pat Inflamm Allergy Drug Discov 12, 39–58.

Yoh, M., Matsuyama, J., Ohnishi, M., Takagi, K., Miyagi, H., Mori, K., Park, K.-S., Ono, T., Honda, T., 2005. Importance of Providencia species as a major cause of travellers' diarrhoea. J. Med. Microbiol. 54, 1077–1082.

Zhong, H., Hu, D.-D., Hu, G.-H., Su, J., Bi, S., Zhang, Z.-E., Wang, Z., Zhang, R.-L., Xu, Z., Jiang, Y.-Y., Wang, Y., 2017. Activity of Sanguinarine against Candida albicans Biofilms. Antimicrob Agents Chemother 61.

527

Table 1(on next page)

MIC of SAG against P. rettgeri

Minimum inhibitory concentration of SAG and antibiotics against seven *P. rettgeri* strains.

1 Table

Stains	MIC(μg/mL)								
	Sang	AMP	FEP	ETP	IPM	TOB	AMK	TZP	F
1#	62.5	>=32	>=64	>=8	>=16	>=16	>=64	>=128	32
2#	62.5	>=32	>=64	>=8	>=16	>=16	>=64	>=128	32
3#	62.5	>=32	>=64	>=8	>=16	>=16	16	64	512
4#	62.5	>=32	>=64	>=8	>=16	>=16	8	>=128	512
5#	62.5	>=32	>=64	>=8	>=16	>=16	8	>=128	512
6#	62.5	>=32	>=64	>=8	>=16	4	<=2	>=128	256
7#	62.5	>=32	16	>=8	>=16	8	4	>=128	256

2

Figure 1

Effects of SAG on the growth kinetics of P. rettgeri cells

Effect of SAG on the growth of P. rettgeri. Bacterial cells were incubated and grown in TBS with 0, 1:8, 1:4, 1, and 2 MIC of SAG at 37°C. Error bars are SD of three replicates.

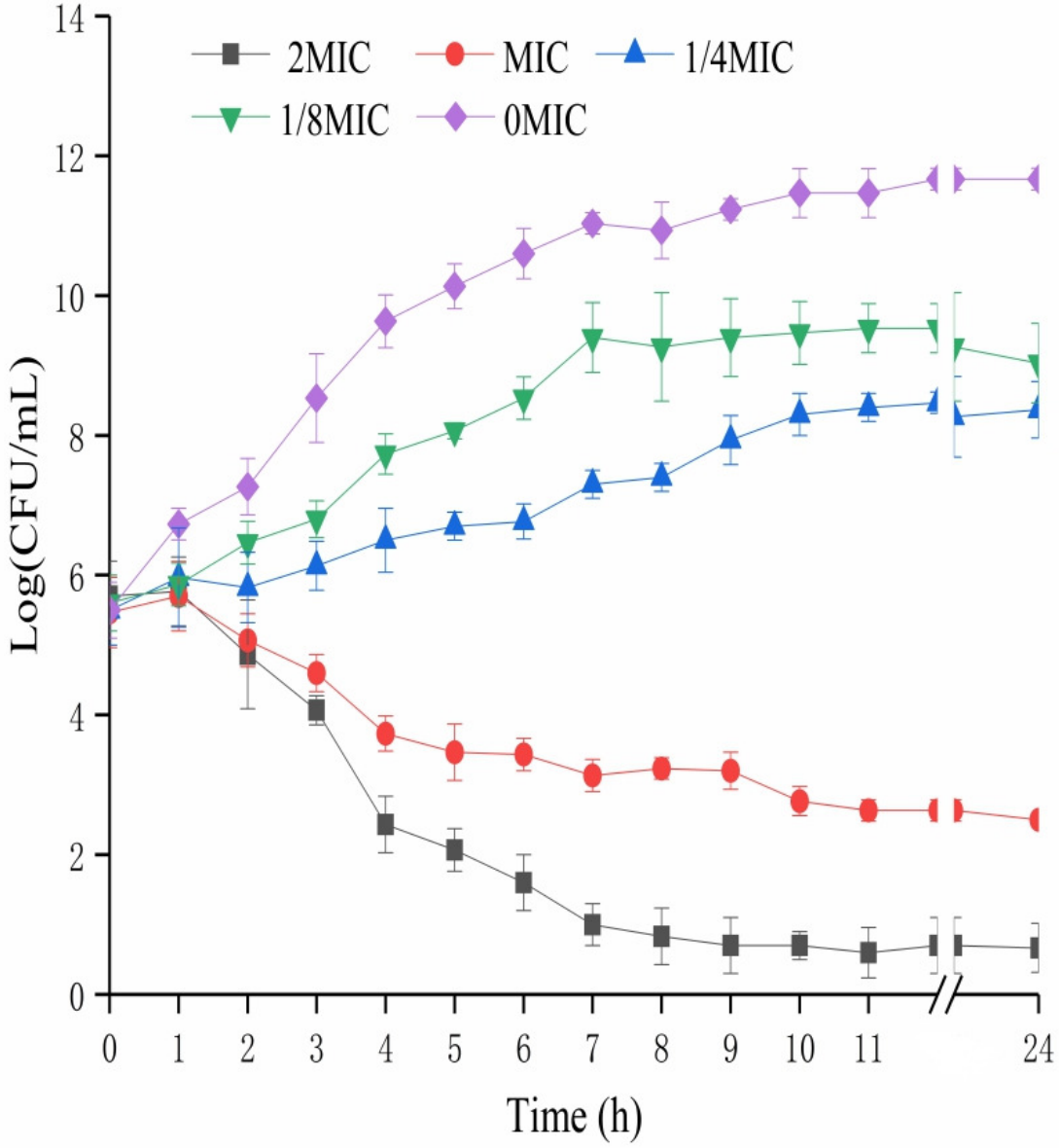
2MIC
MIC
1/4MIC
1/8MIC
0MIC
Log(CFU/mL)
Time (h)
0
2
4
6
8
10
12
14
0
1
2
3
4
5
6
7
8
9
10
11
24

Figure 2

SAG treatment led to a decrease in the intracellular ATP concentrations, pH, and membrane potential of P. rettgeri

Effects of SAG on *P. rettgeri*: (A) intracellular and (B) extracellular ATP levels, (C) membrane potential, and (D) pH_{in}. Data are expressed as mean ± SD. *P < 0.05; **P < 0.01 vs. 0 MIC.

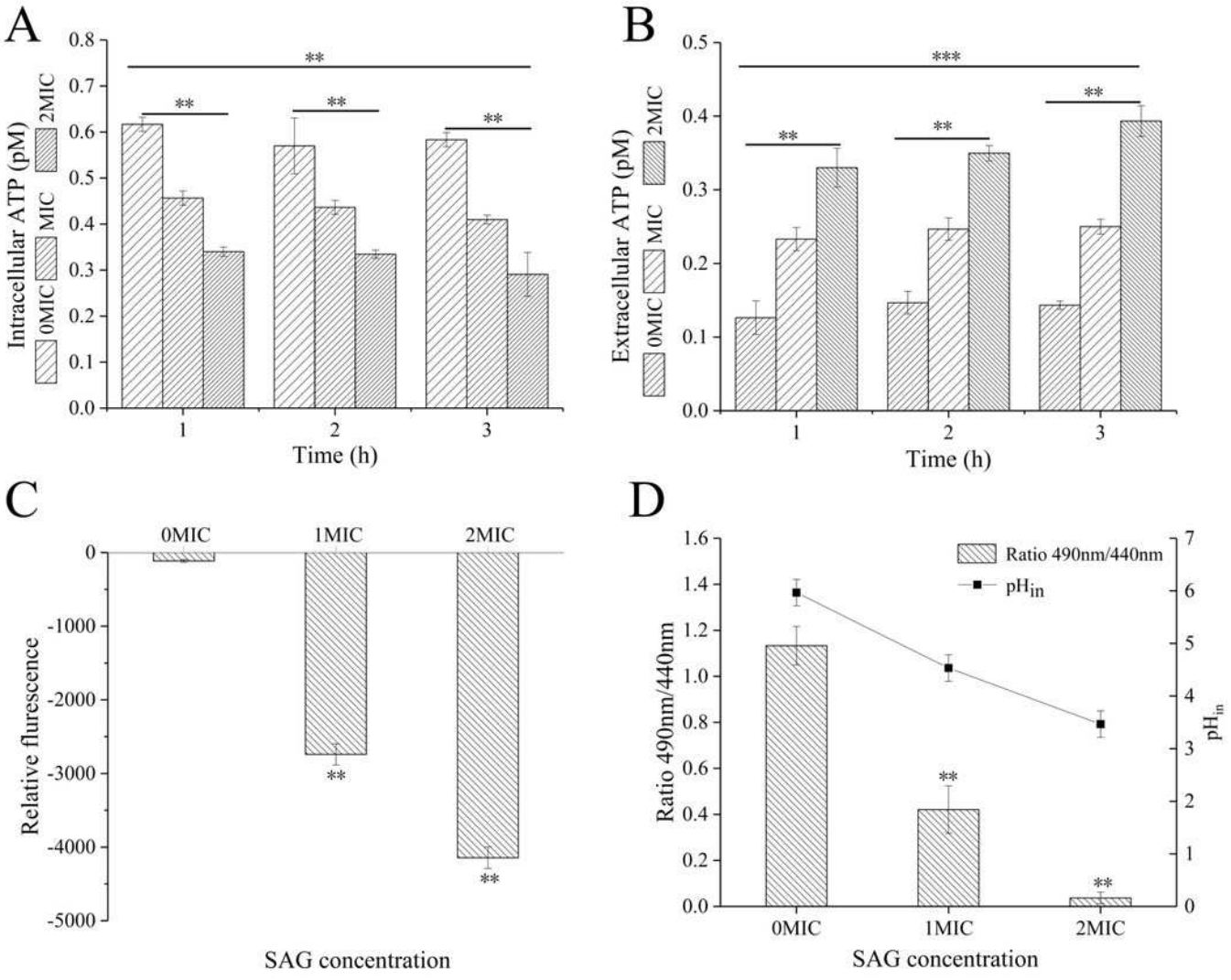

Figure 3

SAG treatment increased the cell membrane permeability of P. rettgeri

Effects of SAG on the cell membrane integrity of *P. rettgeri* cells through CLSM: (A) *P. rettgeri* cells exposed to 1% DMSO, (B) *P. rettgeri* cells exposed to SAG at 1 MIC, and (C) *P. rettgeri* cells exposed to SAG at 2 MIC.

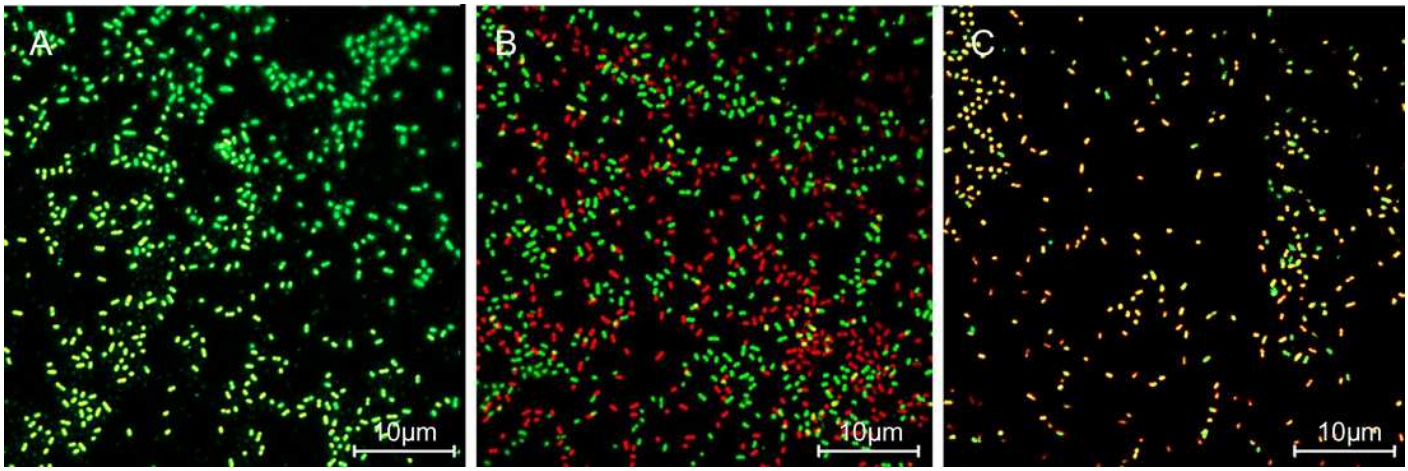

Figure 4

Treatment with SAG led to changes in the cell morphology of P. rettgeri

Effects of SAG on the cell structure of *P. rettgeri* through TEM. (A) *P. rettgeri* cells treated with 1% DMSO, (B) *P. rettgeri* cells treated with SAG at 1 MIC, and (C) *P. rettgeri* cells treated with SAG at 2 MIC.

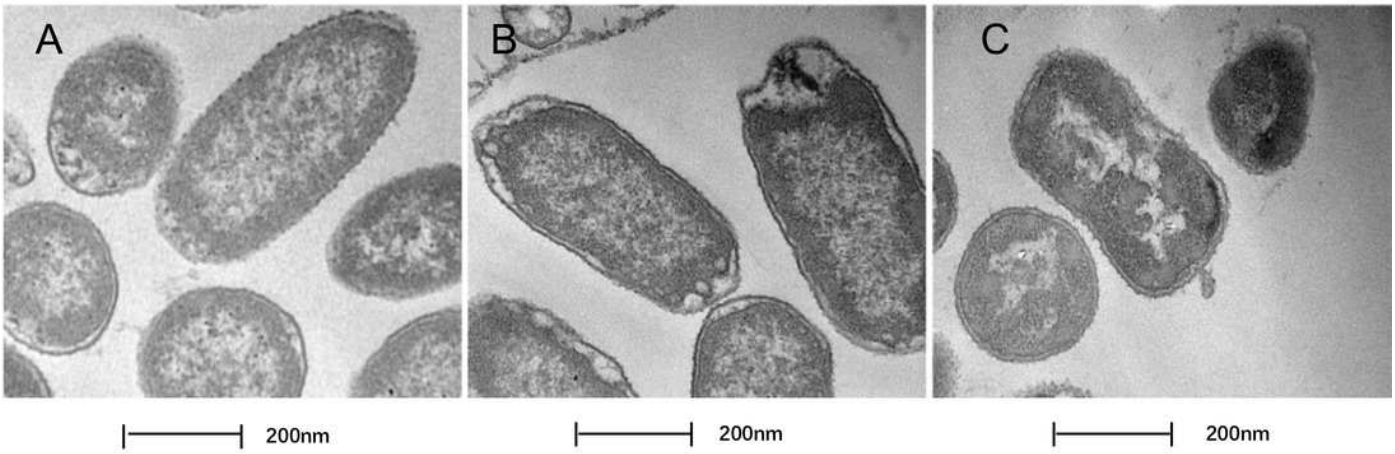

Figure 5

Treatment with SAG led to changes in the cell morphology of P. rettgeri

Effects of SAG on the cell morphology of *P. rettgeri* using FESEM: (A) *P. rettgeri* cells exposed to 1% DMSO, (B) *P. rettgeri* cells exposed to SAG at 1 MIC, and (C) *P. rettgeri* cells exposed to SAG at 2 MIC.

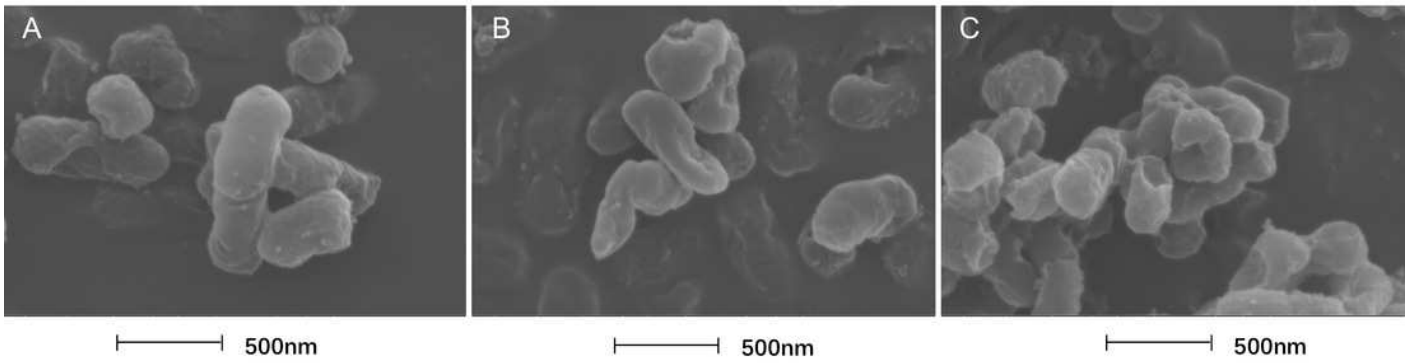

Figure 6

Inhibitory effect of SAG on the biofilm formation of P. rettgeri

Inhibitory effects of SAG on the biofilm formation of *P. rettgeri.* The biofilm formation index was tested by crystal violet staining with different concentrations of SAG in 96-well plates.

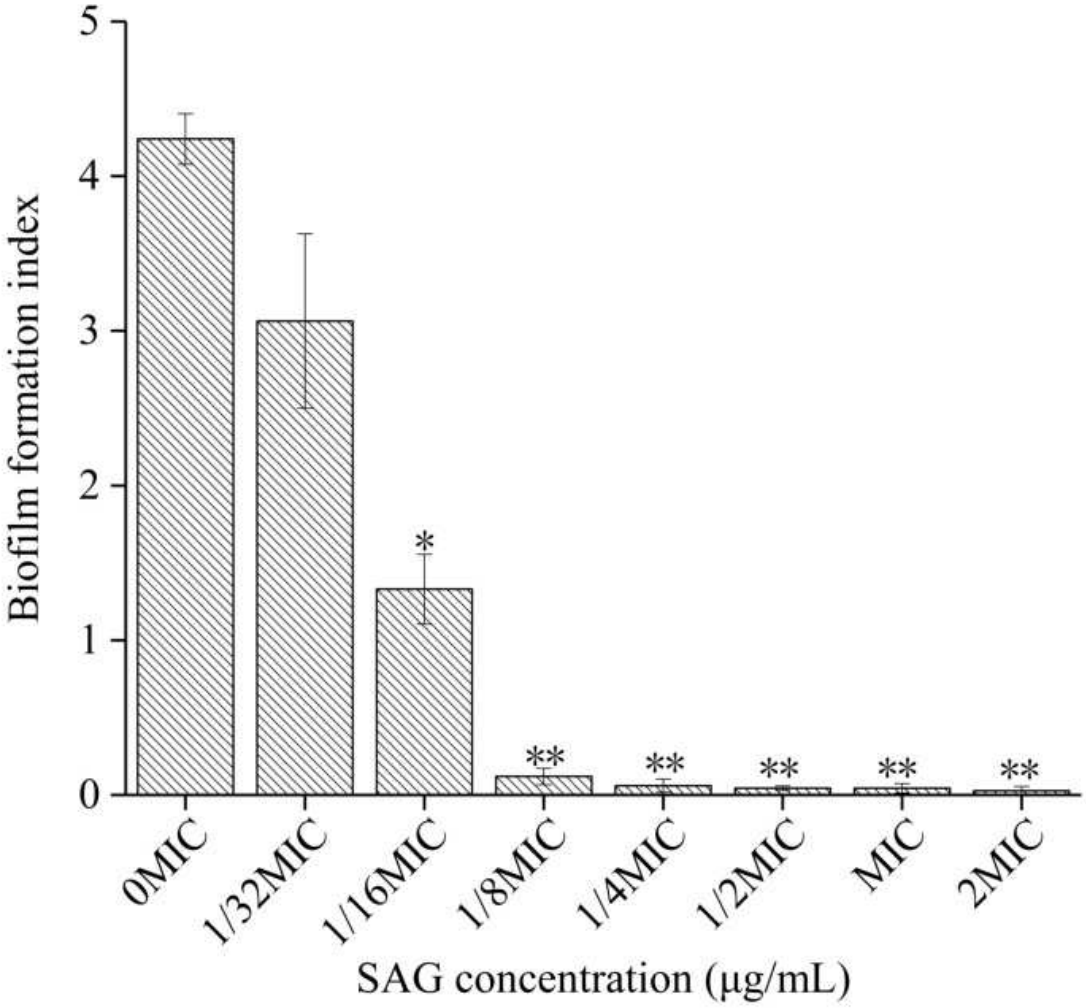

Figure 7

Effect of SAG on the biofilm formation of *P. rettgeri.*

Effect of SAG on the biofilm formation of *P. rettgeri.* Images of FESEM (A–C; magnification, 10,000×) and CLSM (D–F; 3D). (A and D) *P. rettgeri* cells exposed to 1% DMSO, (B and E) *P. rettgeri* cells exposed to SAG at 1 MIC, and (C and F) *P. rettgeri* cells exposed to SAG at 2 MIC.

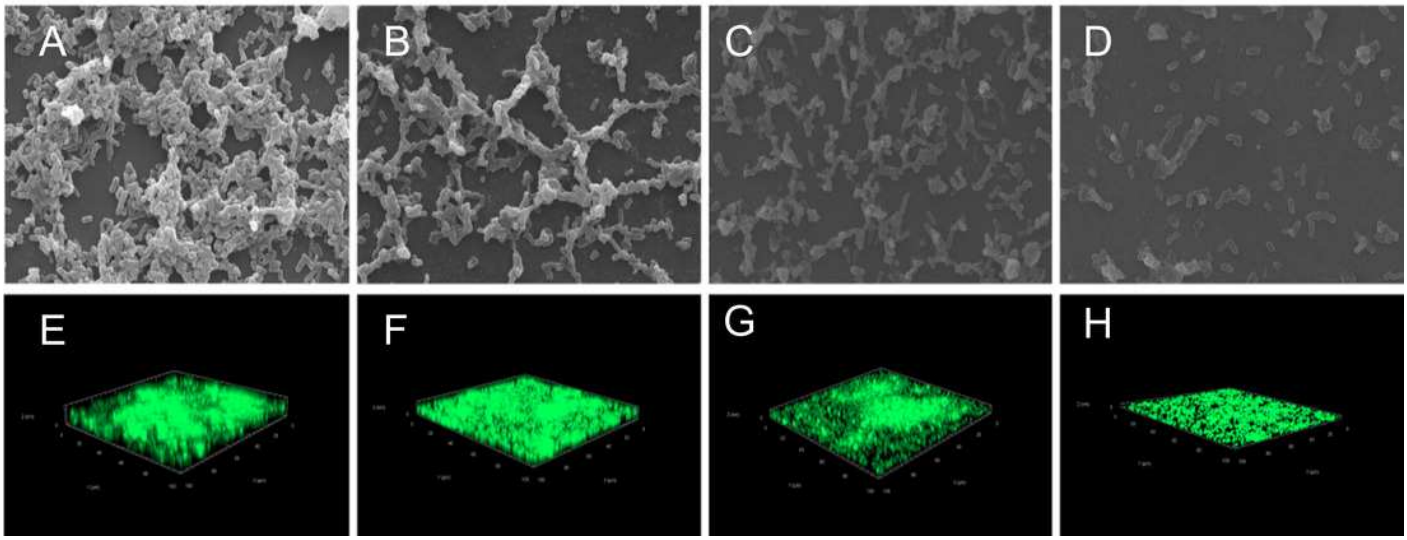

Figure 8

Inactivation effect of SAG on the biofilm of P.rettgeri cells

Inactivation effect of SAG on *P. rettgeri* cells within biofilms. 1D (A–D) and 3D (E–H) images of CLSM. (A and E) *P. rettgeri* cells within biofilms unexposed to SAG. (B and F) *P. rettgeri* cells within biofilms exposed to SAG at 1 MIC. (C and G) *P. rettgeri* cells within biofilms exposed to SAG at 2 MIC. (D and H) *P. rettgeri* cells within biofilms exposed to SAG at 4 MIC.

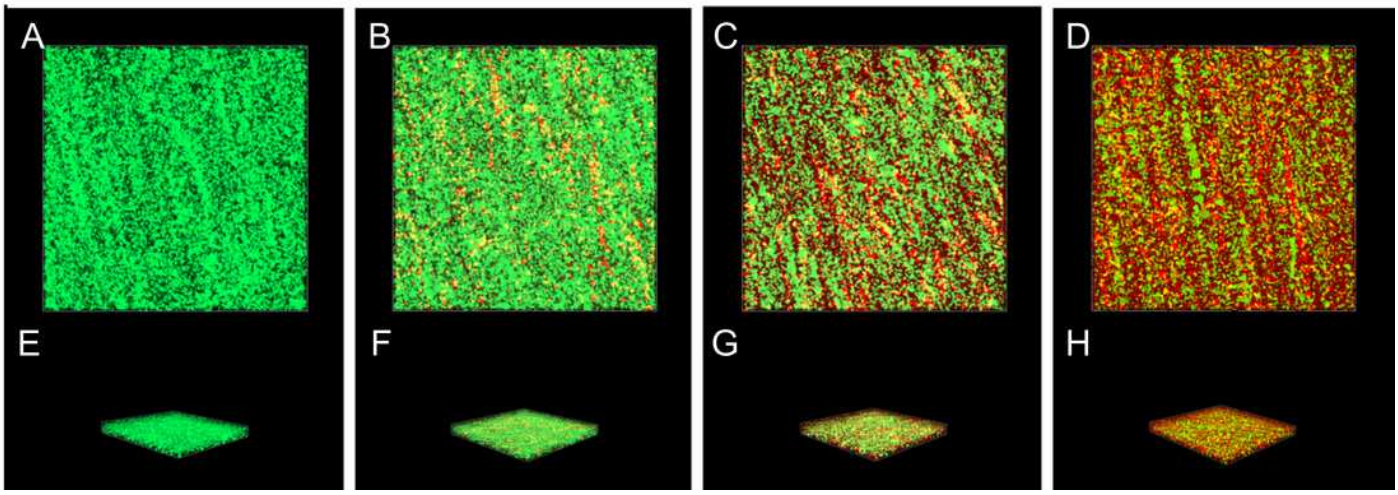

Figure 9

SAG could change the biofilm matrix composition of P. rettgeri cells

Effects of different concentrations of SAG on the levels of carbohydrates, extracellular proteins, and extracellular DNA inside *P. rettgeri* biofilms. (A) eDNA labeled red (PI). (B) Carbohydrates labeled green (WGA). (C) Proteins labeled red (SYPRO Ruby). Scale bar, 10 μm.

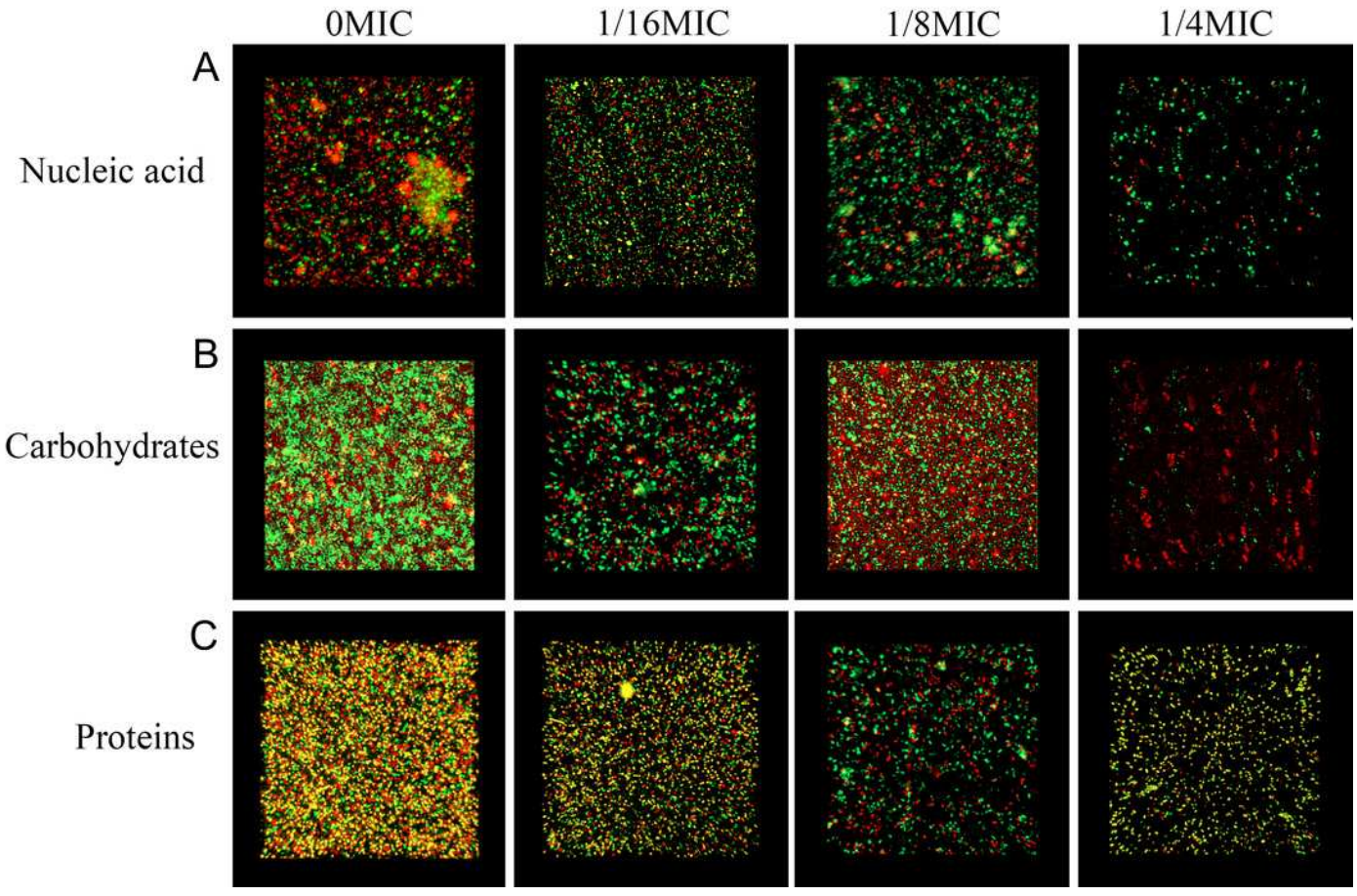

Figure 10

Effect of SAG on biofilms of diffusion

Effect of SAG on biofilms of diffusion. (A) P. rettgeri cells treated with 0 MIC and gatifloxacin. (B) P. rettgeri cells treated with 1:16 MIC and gatifloxacin. (C) P. rettgeri cells treated with 1:8 MIC and gatifloxacin. (D) P. rettgeri cells treated with 1:4 MIC and gatifloxacin.